Supplement of Geosci. Model Dev., 11, 815–842, 2018
https://doi.org/10.5194/gmd-11-815-2018-supplement

Geoscientific Model Development
Open Access
EGU

Supplement of

A fire model with distinct crop, pasture, and non-agricultural burning: use of new data and a model-fitting algorithm for FINAL.1

Sam S. Rabin et al.

Correspondence to: Sam S. Rabin (sam.rabin@kit.edu)

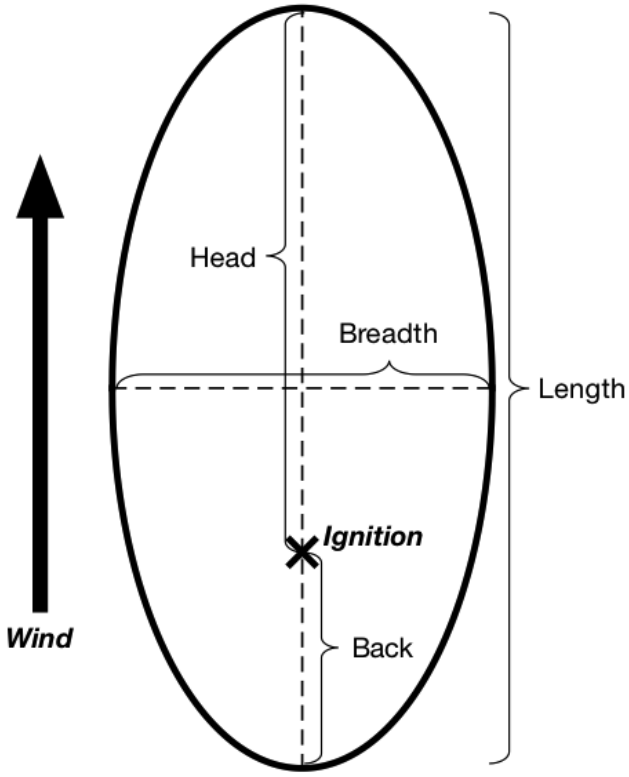

Figure S1. Approximation of fire as an ellipse. Adapted from van Wagner (1969) and Arora and Boer (2005).

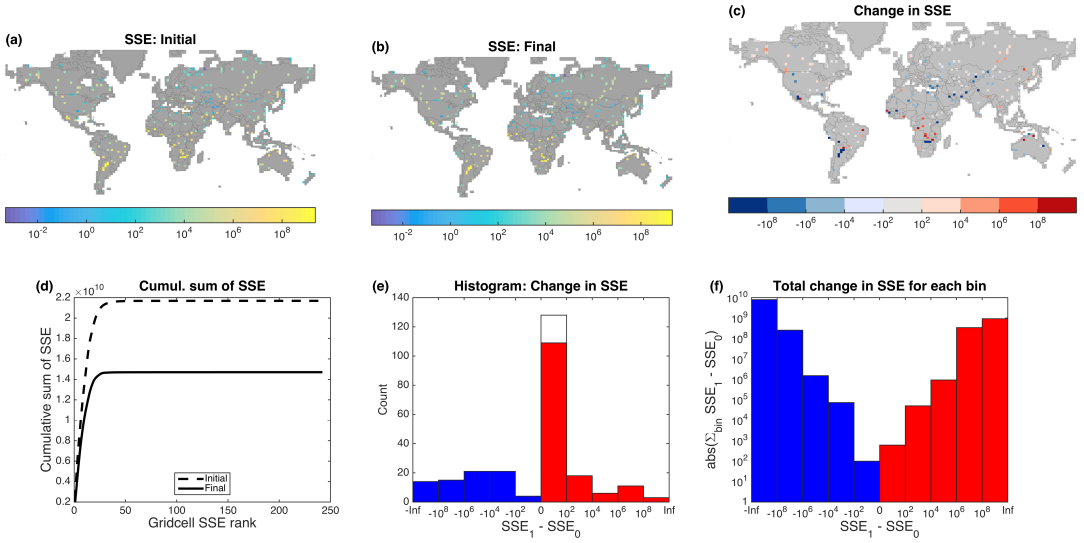

Figure S2. Performance change in gridcells chosen for optimization (Optimization 3). **(a–b)**: Sum of squared errors from model output with initial **(a)** and final **(b)** parameter sets. **(c)**: Difference in sum of squared errors (identical to Fig. 4d, but with non-optimized gridcells masked). **(d)**: Cumulative SSE before and after optimization, with gridcells sorted by SSE descending. **(e)**: Histogram of relative difference in SSE from initial to final parameter sets. Blue represents gridcells that either improved or did not change; red represents gridcells where performance worsened. **(f)**: The total change in SSE for each bin in **(e)**.

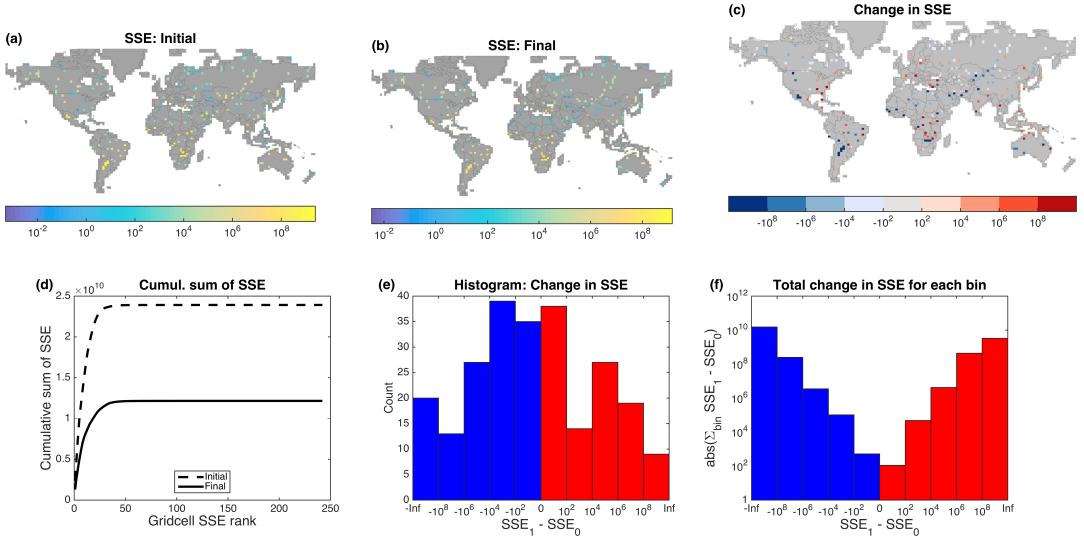

Figure S3. As Fig. S2, but for Optimization 2.

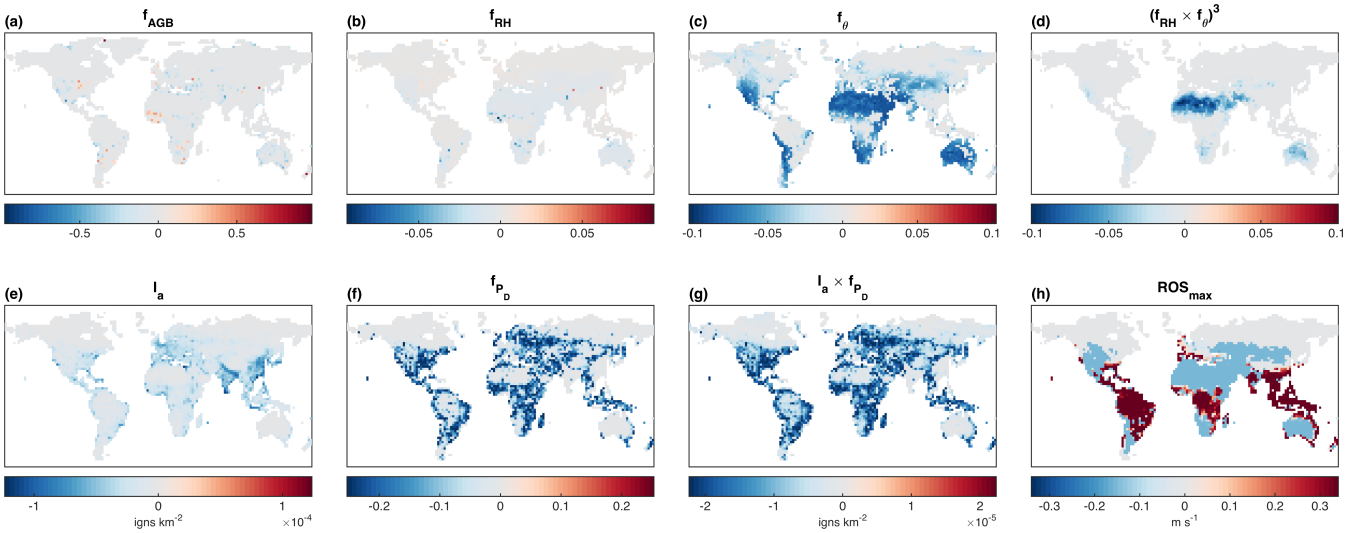

Figure S4. Difference in mean value of various fire model functions over 2001–2009 between `FINAL_V0` and `FINAL_V1` (Optimization 3). Red indicates regions where the function in `FINAL_V1` allows more fire than in `FINAL_V0`; blue, less.

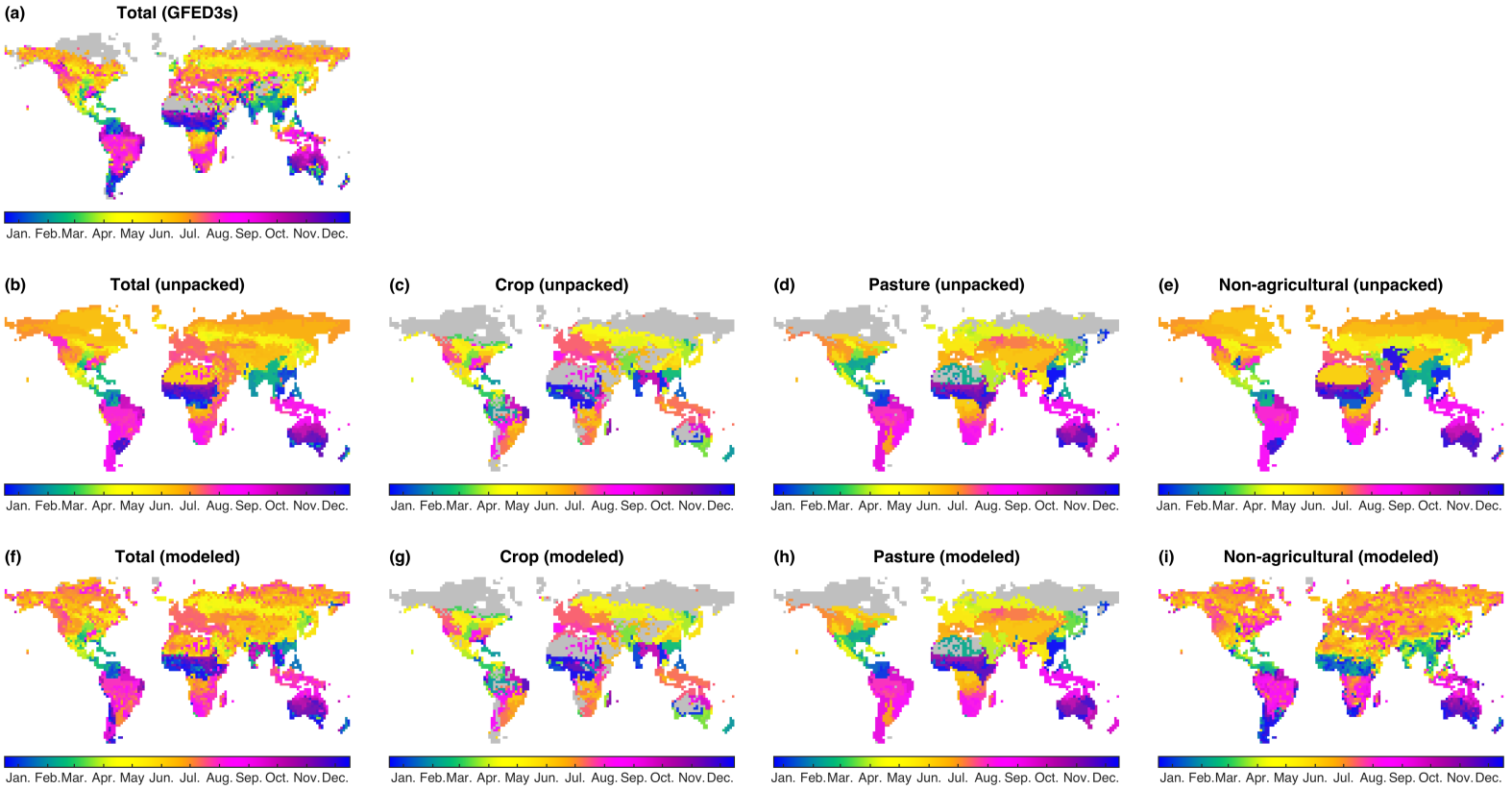

Figure S5. Mean seasonal phase of burned area **(a)**: From GFED3s (Randerson et al., 2012); (B–E): observational estimates from Rabin et al. (2015); (F–I): Model-estimated. Unburned cells in each map are colored gray. Tick marks and labels placed on the 15th of each month. Note that seasonal phase is not necessarily equal to month of peak burned area.

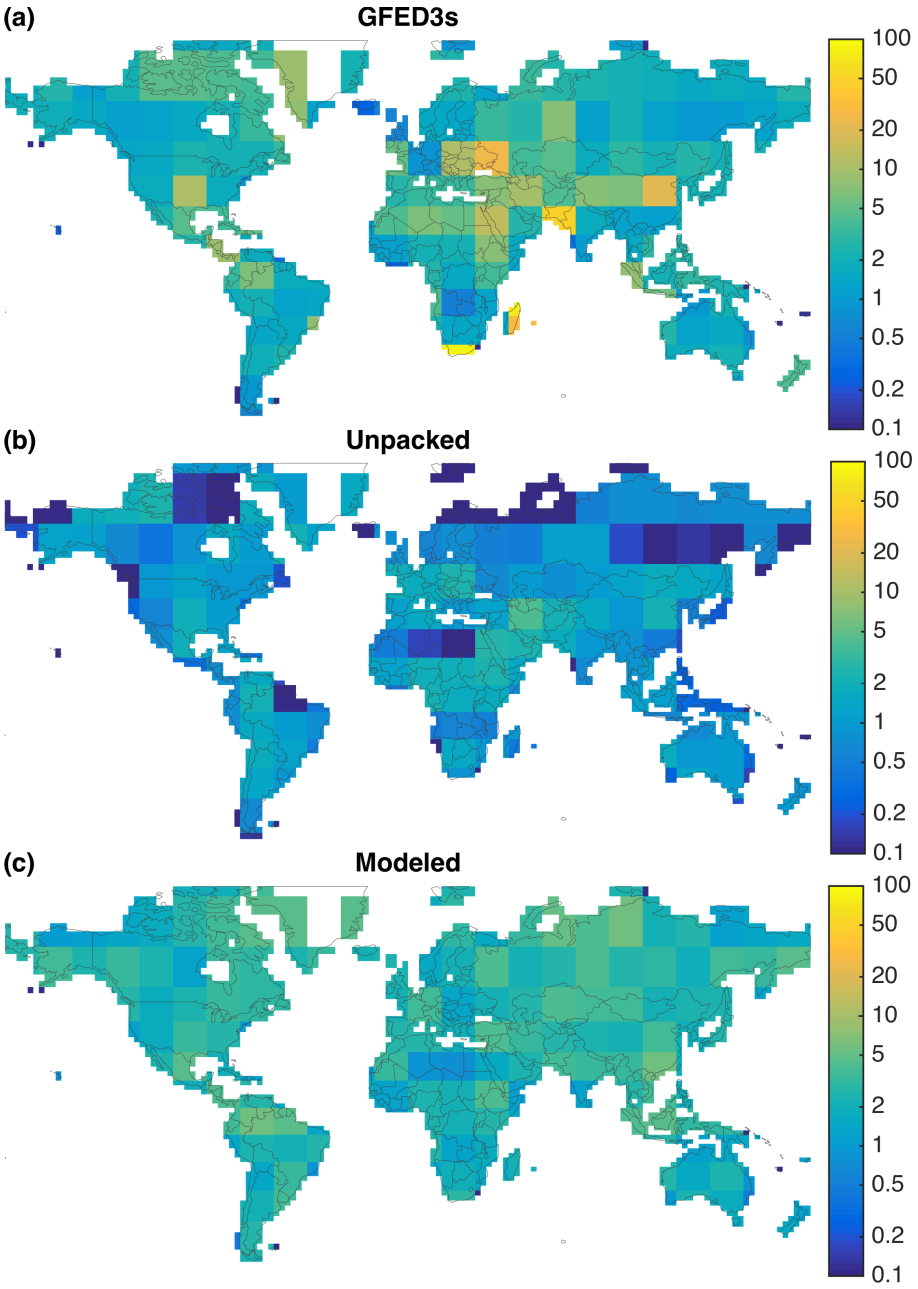

Figure S6. Coefficient of variation (standard deviation divided by mean) of non-agricultural burned fraction in 6×6 gridcell kernels (12° latitude $\times$ 15° longitude). **(a)** Modeled; **(b)** from artificially-constructed GFED3s non-agricultural fire data as described in text; **(c)** unpacked. Note log scale of color bars.

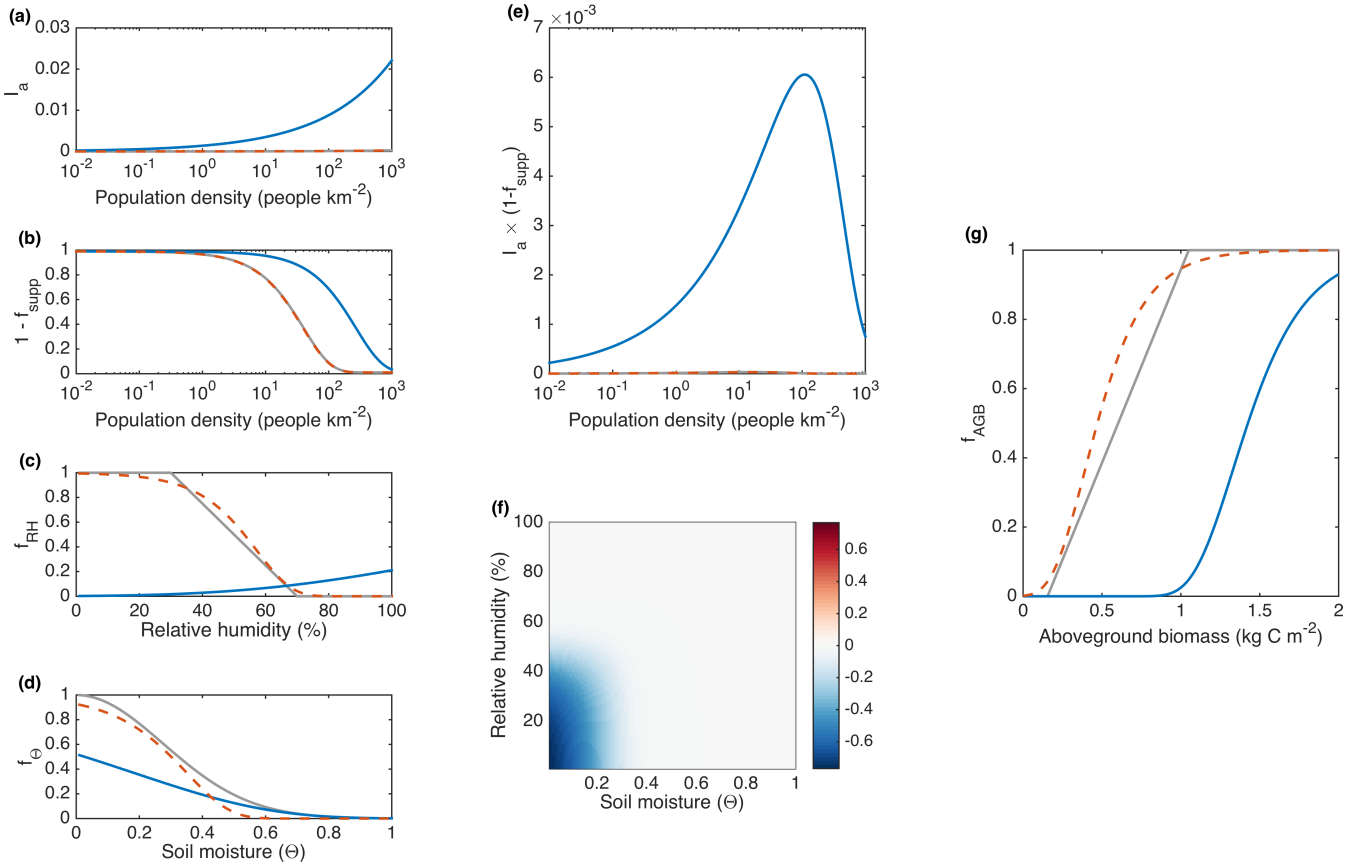

Figure S7. Optimization 2: Changes in functions that were optimized, from original Li et al. (2012, 2013) functions (solid gray) to initial guesses with Gompertz-style functions where necessary (dashed red) to final parameter set (solid blue). Color bar in panel **f** indicates difference in the cubed product of f_θ and f_{RH} (range 0 – 1) between the original and new parameterizations, with blue indicating a lower value in the new parameterization.

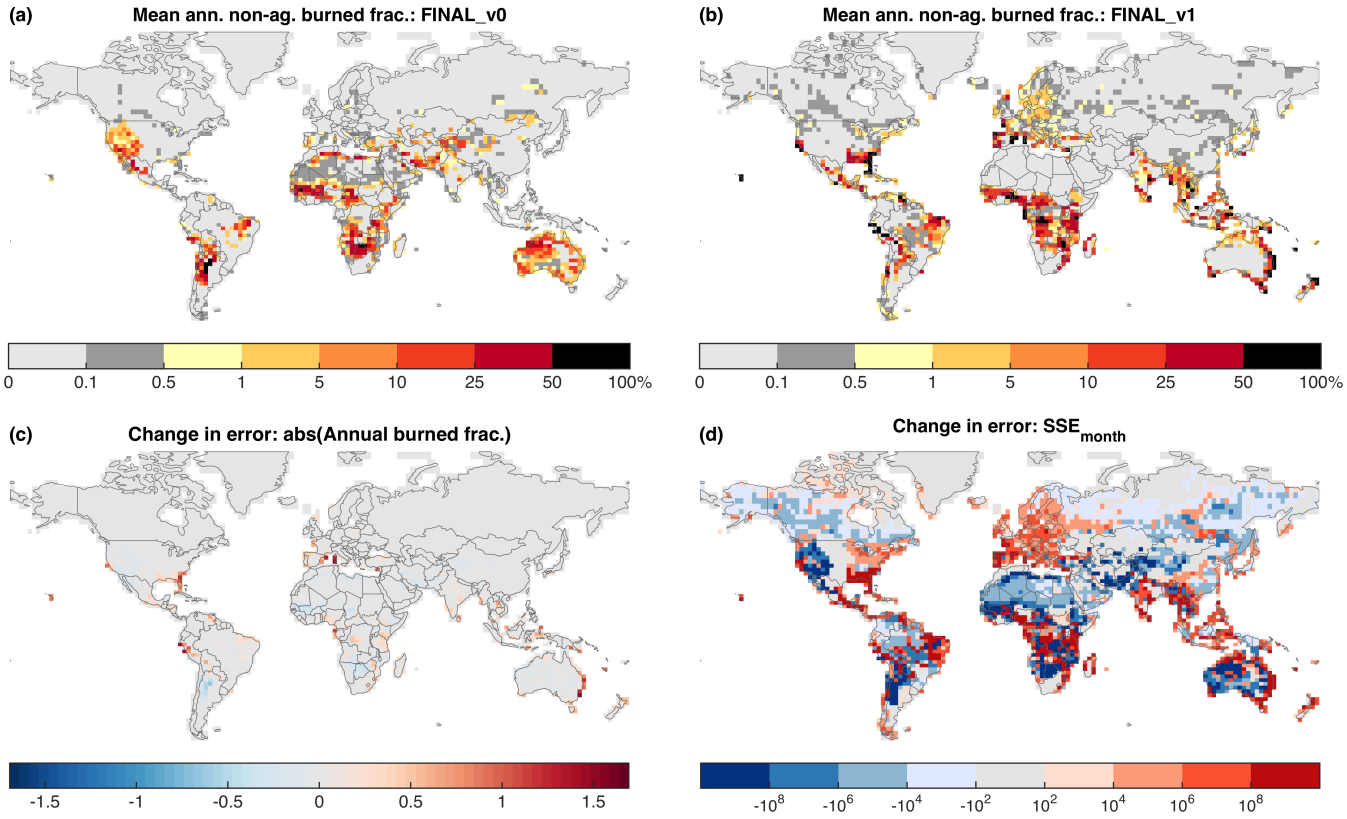

Figure S8. Change in non-agricultural fire model performance for Optimization 2. **(a–b)** Mean annual burned fraction on non-agricultural lands from the initial guess **(a)** and the final parameter set (**b**; identical to Fig. 5i.) **(c–d)** Difference between runs `FINAL_V0` and `FINAL_V1` in correspondence of modeled to unpacked non-agricultural burning (Fig. 5e) as measured by mean annual burned fraction **(c)** and sum of squared errors of burned area evaluated at monthly resolution **(d)**. For **(c)** and **(d)**, blue indicates improvement by `FINAL_V1` over `FINAL_V0`.

Table S1. Initial and final parameter sets for each optimization, at full precision used. Optimization 1 did not complete successfully.

	Initial 1	Final 1	Initial 2	Final 2	Initial 3	Final 3	Initial 4	Final 4
$\beta_{AGB,1}$	7.3157	—	6.6137	188.387124808	6.2754	8.76352843608	6.0616	9.10263711122
$\beta_{AGB,2}$	4.11	—	4.7921	3.93309010451	3.8471	2.68769770241	3.6518	2.53793463318
$\beta_{Ia,m}$	0.0035	—	0.0033	0.299423657595	0.0036	0.00243189648422	0.0041	0.00259814398614
β_{PD}	0.025	—	0.0254	0.00369902210379	0.0218	0.0446640311453	0.0253	0.0509001455347
$\beta_{RH,1}$	0.0062	—	0.0055	6.1731246318	0.0052	0.006922257933	0.0056	0.00686294612402
$\beta_{RH,2}$	-9.1912	—	-9.0809	1.37631745831	-7.5288	-7.14134228066	-6.1629	-5.51016435351
$\beta_{\theta,1}$	0.075	—	0.0763	0.652392803888	0.0866	0.121057112009	0.0905	0.116869508196
$\beta_{\theta,2}$	-6.3741	—	-7.3291	-2.31502528565	-8.4253	-8.10717381374	-9.3429	-9.5275559021
β_{ROStt}	0.3	—	0.3128	1.58857665252	0.3452	0.685455176922	0.4041	0.776114904211
β_{ROSgr}	0.4	—	0.3742	3.13884933876	0.4112	0.26022084993	0.4622	0.292410633937

References

Arora, V. K. and Boer, G. J.: Fire as an interactive component of dynamic vegetation models, Journal of Geophysical Research, 110, 2005.

Li, F., Zeng, X. D., and Levis, S.: A process-based fire parameterization of intermediate complexity in a Dynamic Global Vegetation Model, Biogeosciences, 9, 2761–2780, doi:10.5194/bg-9-2761-2012, http://www.biogeosciences.net/9/2761/2012/, 2012.

Li, F., Levis, S., and Ward, D. S.: Quantifying the role of fire in the Earth system—Part 1: Improved global fire modeling in the Community Earth System Model (CESM1), Biogeosciences, 10, 2293–2314, doi:10.5194/bg-10-2293-2013, http://www.biogeosciences.net/10/2293/2013/, 2013.

Rabin, S. S., Magi, B. I., Shevliakova, E., and Pacala, S. W.: Quantifying regional, time-varying effects of cropland and pasture on vegetation fire, Biogeosciences, 12, 6591–6604, doi:10.5194/bg-12-6591-2015, http://www.biogeosciences.net/12/6591/2015/, 2015.

Randerson, J. T., Chen, Y., van der Werf, G. R., Rogers, B. M., and Morton, D. C.: Global burned area and biomass burning emissions from small fires, Journal of Geophysical Research, 117, G04 012, doi:10.1029/2012JG002128, http://www.agu.org/pubs/crossref/2012/2012JG002128.shtml, 2012.

van Wagner, C. E.: A simple fire-growth model, The Forestry Chronicle, 45, 103–104, doi:10.5558/tfc45103-2, https://cfs.nrcan.gc.ca/publications?id=33478, 1969.